Deep Dense Model for Classification of Covid-19 in X-ray Images

Wesam H. Alsabban[1], Fareed Ahmad[2], Ali Al-Laith[3], Saeed M. Kabrah[4], Mohammed A. Boghdadi[5], Farhan Masud[6]

[1]Information systems department, Faculty of computer and information systems, Umm Al-Qura University, Makkah, Kingdom of Saudi Arabia.

[2]Quality Operations Laboratory, Institute of Microbiology, Faculty of Veterinary Science, University of Veterinary and Animal Sciences, Lahore, Pakistan

[3]Center for Language Engineering, Alkhawarizmi Institute of Computer Science, University of Engineering and Technology, Lahore, Pakistan

[4]Laboratory Medicine Department, Faculty of Applied Medical Sciences, Umm Al-Qura University, Makkah, Kingdom of Saudi Arabia.

[5]King Faisal Specialist Hospital and Research Centre (KFSH&RC) Jeddah, Kingdom of Saudi Arabia.

[6]Department of Statistics and Computer Science, Faculty of Life Sciences Business Management, University of Veterinary and Animal Sciences, Lahore, Pakistan

Summary

Novel Coronavirus, SARS-CoV-2, can be fatal for humans and animals. The ease of its propagation, with its extraordinary ability to cause disease and even death in humans, makes it a hazard to humanity. Chest X-ray is the most popular but difficult to apprehend radiographic analysis for immediate diagnosis of COVID-19. It yields significant anatomical and physiological information. However, extracting the appropriate information from it is seldom difficult, even for radiologists. Deep CNN architectures can assist in reliable, swift, and accurate results. We propose a deep dense model fine-tuned from scratch and statistically analyzed its results using paired two-sided t-test with state-of-the-art deep learning models, namely, SqueezeNet, AlexNet, DenseNet201, and MobileNetV2. Current datasets are limited and generally unbalanced. However, we devised a larger and well-balanced dataset for training the model. Moreover, as the dataset is still not significant, thus data augmentation and fine-tuning approaches are employed to evade overfitting and generate a better-generalized model. Our deep dense model produces better performance from analyzed deep learning models to generate Specificity, Recall, FScore, and Accuracy of 97.33%, 92.01%, 92.00%, and 96.01%, when trained on a significantly larger and balanced dataset, while employing 5-Folds cross-validation. The statistical analysis also shows that our model is better than its competing methods. Our deep model can help radiologists in the correct identification of COVID-19 in X-rays.

That can contribute toward speedy and reliable diagnosis, thereby saving precious lives and minimizing the socio-economic burden on society.

Key words:

Deep learning models, dense model, fine-tuning, augmentation, transfer learning, COVID-19 classification, coronavirus.

1. Introduction

Microbes cause many zoonotic diseases, which are transmitted from animal to humans [1]. The effects of such diseases present a risk not only to human and animals but also to world health safety [2]. About 1500 microbes are known to cause infections in human beings [3]. About 61% of the documented and 75% of the evolving contagious infections in the community are zoonotic [2, 4]. Moreover, 16% of the mortalities and 44% of the deaths in underdeveloped nations caused by infectious diseases [2]. Zoonotic diseases induce 2.7 million mortalities and 2.5 billion infections in the society [5]. The evolving zoonotic illnesses are liable for numerous high-level pandemics [6].

COVID-19 is a zoonotic disease that transfers to humans through bats or pangolins [7, 8]. There exists no direct relation among human beings and various other species. As the virus is a mutated microbe, it can conveniently cross the specie barrier and affects human respiratory tract [9,10]. As a result, the virus can cause kidney malfunction, acute respiratory infections and pneumonia, and can also cause mortalities [11]. The virus can survive in aerosol form and on numerous surfaces from many hours to several days [12]. The research reports that the virus propagates either by exhaled or sneezed or coughed droplet particles of 5 to 10 μm and around thirty times smaller than the diameter of a human hair. [12,13]. Experts report in [14,15] that the pathogen can exist in the air as droplets. WHO is presently evaluating the role of aerosols in transmission [16]. The organization informed that the virus can prevail in closed, crowded, and poorly ventilated environments [17]. Research [18] reports that sneeze can cause the droplets of the pathogen to travel up to 27 feet. Its capacity to prevail and propagate in the environment and infect and even cause mortality in individuals makes it a probable contestant for biological warfare [19–21]. The epidemic is extensively widespread in the USA, UK, and Europe. Millions of individuals got infected, and thousands have lost their lives due of the virus. Globally, as of 24 September 2021, there were 230 million infections and 4.7 million reported deaths. In the US, there were 42 million positive cases and 0.48

Manuscript received January 5, 2022
Manuscript revised January 20, 2022
https://doi.org/10.22937/IJCSNS.2022.22.1.56

million deaths. The virus may cause 2.4 million mortalities in the US if proper safety measures are not initiated [22, 23]. In the United Kingdom and the EU states such as France, Germany, Spain, and Italy about 15.88 million people were infected, and 0.34 million died [22]. The UK's health officials maintain that the infection can affect 80% of the community, and 0.5 million mortalities are expected [24]. Overall, billions of individuals are in self-quarantine or under lockdowns. If the pathogen is permitted to propagate at this speed, the primary-care setup will be overwhelmed, markets will crumble, and valuable human lives could be wasted [23, 25].

RT-PCR and ELISA are the generally accepted methods for the classification of COVID-19 [26]. RT-PCR, which detects the pathogen's RNA from respiratory tract samples, is the key screening approach for distinguishing COVID-19. Swabs from the nasopharyngeal or oropharyngeal regions are used to obtain these samples. While RT-PCR is considered the gold standard [27, 28], it is a tedious, complex, and sensitive standard procedure [29]. Sample errors, low sensitivity, and low viral load can also impact test results [30, 31]. The test results can be falsely negative if the viral load is insufficient [28, 32]. Chest radiographs like CT-Scan and X-rays are an alternative approach for COVID-19 screening. Experts examine these radiographs to evaluate the likely lesion associated with COVID-19. Primary researches reveal that individual infected with COVID-19 exhibit abnormalities in chest radiographs [28, 33]. Recent researches infer that radiological analysis can be adopted as a primary tool for virus detection in affected areas [28]. Radiographic examinations can be executed instantly and are easily available in our primary health infrastructure. It is a true compliment to the PCR test (in few instances even exhibiting greater sensitivity) [28, 32]. The main problem with X-ray analysis is that they need an experienced expert to evaluate the radiograph image, as visual signs are hard to infer [34,35]. However, computer-aided models can assist radiologists interpret X-rays precisely and instantly to identify chest abnormalities that cause coronavirus infections.

Currently, deep learning designs can expedite speedy diagnosis, rapid prevention, and elimination of contaminations induced by coronavirus [36]. A fusion of deep models (for example, InceptionV3 [37] and AlexNet [38]), open-source databases (for example, ImageNet [39]), and an efficient overfit checking procedure (for example, Dropout [40]) has demonstrated enhanced performance, accuracy, and excellent generalizability to resolve pathological [41, 42], biological [36,43], and complicated computer-vision endeavor's [44]. The benefit of CNN models for computer vision tasks is that a design is trained from start to end but undergoes overfitting with minute datasets. For deep networks, it is difficult to attain the same magnitude of performance with small datasets as with large datasets [45]. The solution to the problem is transfer learning [46], which replaces few last layers of a deep model and fine-tune it on a distinct dataset. The method is helpful when augmentation [44] with suitable hyper-parameters and efficient fine-tuning tactics are employed. Next, we present the overview of the latest research related to COVID-19.

Image processing and CNN models have displayed promising outcomes, especially in the field of chest radiographs. These routines carry lung nodule identification [47], pulmonary tuberculosis classification [48], and specially for COVID-19 analysis [35, 49, 50, 51, 52].

Xu et al. [51] propose a 3 category framework to distinguish among viral, normal, and coronavirus examples. The method is based on segmentation that achieves almost 87% accuracy with 618 CT images. Wang et al. [52] propose a deep learning model to attain visual features from CT images for coronavirus identification. The model consists of 1,065 CT images (325 coronavirus and 740 viral) of individuals, which achieves an accuracy of 79.3%. Gozes et al. [53] present a rapid AI base development cycle applying CNN's for CT image analysis.

Ioannis et al. [54] present a deep learning approach to classify different chest infections with 224 COVID-19, 504 normal, and 700 bacterial images. The model achieves a specificity, accuracy, specificity, and sensitivity of 96.46%, 98.66%, and 96.78%, respectively. Although the approach analyzed the outcomes of different models, the results rely on a limited number of coronavirus images. In ref. [35] the scholars contribute a pooled open-source dataset and propose a COVIDNet model for the classification of coronavirus, which uses chest radiographs as input. The dataset comprises 5538 pneumonias, 358 COVID-19, 8066 normal radiographs. The model attains an accuracy of 93.3%, but like previous approaches, the model relies on limited COVID +ve images. Ucar and Korkmaz [55] use SqueezeNet deep model while employing Bayesian optimization approach to distinguish coronavirus infections in chest radiographs. The dataset consists of 3,895 pneumonia, 66 COVID-19, and 1,349 normal radiographs. Although the strategy reveals inspiring outcomes on a minute dataset, its results need verification on a larger dataset. Abbas et al. [56] propose a convolutional design that exhibits dimensionality reduction and transforms a high-resolution image into a lower-dimensional feature space. It consists of 11 SARS, 80 normal, and 105 COVID-19 radiographs. The design accomplishes almost 95% accuracy. Khan et al. [57] apply the Xception architecture to distinguish COVID-19 infections in chest radiographs. It consists of 327 viral, 284 COVID-19, 310 normal, and 330 bacterial images. For limited data instances, the design accomplishes an accuracy of 89.6%, while the combination of the two classes (bacterial and viral pneumonia) achieves an accuracy of 95%. Ashfar et al. [58] propose a capsule-based network known as COVIDCAPS. The model attains 95.7% accuracy in 94,323 radiographs associated with common chest diseases. Gian-chandaniet al. [59] employ two deep networks, one consisting of ResNet152V2 and VGG16 for binary classification (normal, COVID19) and

the other comprising of DenseNet201 and VGG16 for three-class identification (virus, COVID19, and bacteria). Each class in binary classification consists of 1525 images, and for three classes, there are only 401 images in each category. However, the results are promising but may not replicate for a significantly larger dataset with numerous classes. The approach applied a simple data split comprising of train, test, and validation sets. However, cross-validation is more feasible for small datasets. Singh et al. [60] apply genetics and particle swarm optimization employing deep architectures for the screening of individuals with COVID-19. These architectures employ a binary classification procedure; they are slow to converge but still give acceptable outcomes. Hyper-parameters are tuned to increase the architecture's performance. The author [61] employs ensemble learning via three deep architectures (ResNet152V2, DenseNet201, and VGG16) on CT images to produce outstanding outcomes on a significantly larger

Table **1.** Comparison of Various Approaches applied for COVID-19 Classification

Approach	**Classes**	**Dataset Description**	**Augmentation?**	**Balanced Dataset?**	**Hyper-parameter Tuning?**	**Statistical Comparison?**	**5-Folds CV?**
[30]	5	C-19 180, N 191, B 54, V 20, T 57	✓	×	✓	×	×
[35]	3	C-19 180, P 6012, N 8851	✓	×	×	×	×
[55]	3	C-19 66, P 3895, N 1349,	✓	×	✓	×	×
[58]	5	Not stated	×	×	×	×	×
[59]	3	C-19 401, N 401, V 401	✓	×	✓	×	×
[62]	3	C-19 183, P 5521, N 8066	✓	×	×	×	×
[63]	3	C-19 99, P 9579, N 8851	✓	×	×	×	×
[64]	4	C-19 313, UP 6012, N 7595, B 2780	×	×	✓	×	×
[65]	2	C-19 184, N 500	✓	×	×	×	×
[66]	4	C-19 68, N 1203, V 660, B 931	✓	×	×	×	×
[67]	3	C-19 423, V 1485, N 1579	✓	×	×	×	✓

The class column presents the total categories in a dataset. Where C-19, P, UP, N, B, V, T, represent the total instances of Covid-19, Pneumonia, Pneumonia of Unknown type, Normal, Bacterial, Viral, Tuberculosis, examples respectively.

four categories (pneumonia, COVID-19, normal, and tuberculosis) dataset. A conventional test\train split is initiated in its place of cross-validation.

(v) We also assess the performance of the proposed design, statistically by applying paired II-sided t-test and 5-Folds CV (Cross-validation).

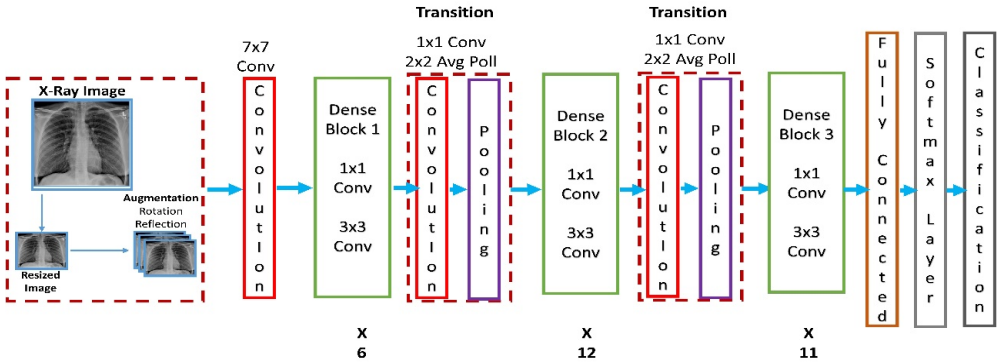

Fig. (1). Various stages of the proposed Deep dense model

Most of the above COVID-19 classification approaches apply machine and deep learning techniques with augmentation, fine-tuning strategies. The dataset in these approaches is unbalanced with limited COVID-19 images that may not generate substantial results on a large dataset. Hyper- statistical analysis, cross-validation, and parameter tuning are also not applied by most researchers. Table 1 summarizes the various research strategies applied for COVID-19 classification using CNN architecture's. In the current work, we devise a comparatively larger and balanced dataset comprising four classes (normal, COVID-19, bacterial, and viral). These images are analyzed by employing fine-tuning with transfer learning on pre-trained deep learning models to demonstrate if these deep models can render more reliable outcomes when data is limited. We also implemented regular data augmentation practices like reflection and rotation [68] which, help resolve the issue of limited data instances by supplementing them with altered original instances. Lastly, we present a deep dense model comprised of Dense blocks with convolution pooling layers, as presented in Fig. 1. The model delivers better results than various deep learning models. Our research contributions are summarized in the following paragraph:

(i) A well-balanced and significantly larger dataset if prepared to comprise of four categories (viral, normal, bacterial, and COVID19). In each category, there are 1200 instances.
(ii) The work unifies various approaches (fine-tuning, hyper-parameter tuning, and augmentation) in one model.
(iii) The work presents a deep model with dense blocks used as the main component of our architecture.
(iv) The Performances of various deep designs are compared with the proposed deep dense model in terms of accuracy, F-Score, recall, and specificity.

Table **2.** The detail design of Deep dense

Layers	**Output Size**	**Proposed Model**
Convolutional layer	112 x 112	stride-2, 7 x 7
Pooling layer	56 x 56	stride-2, 3 x 3 Max-pool
Dense (block-1)	56 x 56	$\begin{bmatrix} 1 \times 1\ conv \\ 3 \times 3\ conv \end{bmatrix}$ x 6
Transition (layer-1)	56 x 56	1 x 1 convolution
	28 x 28	stride-2, 2 x 2 Average-pool
Dense (block-2)	28 x 28	$\begin{bmatrix} 1 \times 1\ conv \\ 3 \times 3\ conv \end{bmatrix}$ x 12
Transition (layer-2)	28 x 28	1 x 1 convolution
	14 x 14	Stride-2, 2 x 2 Average-pool
Dense (block-3)	14 x 14	$\begin{bmatrix} 1 \times 1\ conv \\ 3 \times 3\ conv \end{bmatrix}$ x 11
Classification Layer	1 x 1	7 x 7 Average-pool
	4	4D fully-connected, softmax

The dataset comprises X-ray images about four different classes(Normal, Viral, Bacterial, and COVID-19). The dataset consists of 4800 images, with 1200 images in each category.

The normal, viral, and bacterial images are retrieved from the Kaggle dataset. [69]. The COVID-19 images are from four sources, 900 images are from Mendeley open-source dataset [70], 200 images are from King Faisal Specialist Hospital and Research Centre [71], and the remaining radiographs are from SIRM [72] and Radiopaedia [73].

Augmentation is applied to augment the volume of the dataset for training, which helps in handling overfitting. Various augmentation routines are for training the model. Which are as follows:

(i) Random horizontal reflection, (ii) Random vertical reflection, (iii) Random vertical shear, (iv) Random horizontal shear, and (v) Random rotation. During training, 80% of the data is for training and 20% is for testing the design.

2.2. Preprocessing

The chest radiology images are large, with several radiographs with a size of 1013 × 1016 pixels. These radiograph images need resizing, so they are adjusted according to the input size of the models. Different models have different input-size such as Densenet201 has an input size of 224-by-224. Cropping further helps in improving the quality by removing the extended black background from the X-ray images.

2.3. Tuning Hyper-parameters

In this research, we examined the effect of numerous hyper-parameters on the results of the chosen deep CNN models. The hyper-parameters are as follows: (i) Epochs, (ii) Batch size, and (iii) Learning rate. These hyper-parameters are applied to different models (SqueezeNet, DenseNet201, AlexNet, and MobileNetV2). During training, numerous variations of these hyper-parameters are used for each CNN model, as shown in table 3. The experimentation shows that these models display the most favorable results with a batch size of 24, 32, and 48. In the beginning, smaller learning rates have shown better results like 1e-6, 1e-7, and 1e-8.

Table **3.** The detail of learning rate and batch size for various Pre-trained models

CNN Network	Batch-size	Learning rate
Alex Net	48, 16 32, 24	5e-10, 7e-5, 1e-5, 8e-7, 1e-8, 1e-7, 6e-7, 1e-6, 5e-4, 1e-4
Squeeze Net	48, 16, 32, 24	1e-7, 1e-4, 1e-8, 9e-4, 8e-7, 9e-5, 1e-6,
MobileNetV2	48, 16, 32, 24	6e-4, 1e-8, 1e-4, 6e-7, 5e-6, 4e-7, 1e-7, 9e-6, 3e-6, 1e-6, 8e-5
DenseNet201	48, 16, 32, 24	1e-4, 1e-7, 1e-6,1e-5

2.4. Convolution neural network (CNN)

The convolution network relies on a traditional neural network and normally comprises of three kinds of layers (convolution, pooling, and a fully-connected layer). Subsequent to the convolutional operation, generally a pooling operation is performed, which reduces dimensionality. This permits us to minimize the parameters, lowers the training time, and also supports in handling overfitting. The pooling down-samples each feature map while preserving the vital features intact. Afterward, the fully connected layer tries to gain a mid-level feature map. Executing full connection in these layers demand a significant number of weight parameters. For additional details, please refer to [74]. The Convolution network operates in a feed-forward fashion; it starts from the primary layer to the terminal layer. The error is propagated in the backward direction, which originates from the terminal layer to the convolutional layer. Let i be a neuron in layer c, which receives data from a neuron j of layer c − 1 in the forward-pass. The input [75] is calculated as follows:

$$\boldsymbol{ln_i^c = \sum_{j-1}^{n} W_{ij}^c + b_i} \quad \textbf{(1)}$$

Where $\boldsymbol{W_{ij}^c}$ $\boldsymbol{and}$ $\boldsymbol{b_i}$ are weight vector and bias-term of the c^{th} layer. ReLU a rectified linear activation method [75] can be utilized to calculate the output, as follows:

$$\boldsymbol{Out_i^c = Max(0, ln_i^c)} \quad (\mathbf{2})$$

The hidden nodes in the convolutional and fully connected layer use Equations (1) and (2) to calculate the input and output. SoftMax [76] is used to compute the classification probability of each pathogen in the terminal layer, as follows:

$$Out_i^c = \frac{e^{ln_i^c}}{\sum_k Out_k^c} \quad (\mathbf{3})$$

Back-propagation is utilized for training the convolution network. It help's in minimizing the cost equation [76] associated to the unknown weight W, as given below.

$$C = -\frac{1}{m}\sum_{n=1}^{m} ln(p(y^n|X^n)) \quad (\mathbf{4})$$

Where m denotes the examples in a training set, X^n is the n^{th} example in the training set and y^n is its corresponding label and its true classification probability is $p(y^n|X^n)$. By means of SGD over the mini-batch's of magnitude N, the cost function is decreased and training costs are assessed by the mini-batch cost. If W^s represents the weights at iteration s for the convolution layer c and C is the cost of mini-batch, the weights [76] are updated at the successive iteration as follows:

$$\gamma^s = \gamma^{\left[\frac{sN}{m}\right]}$$

$$V_c^{s+1} = \mu v_c^s + \gamma^s \alpha_c \frac{\partial C}{\partial W_c}$$

$$W_c^{s+1} = W_c^s + V_c^{s+1}$$

Where layer c's learning rate is represented as α_c .The symbol γ denotes scheduling rate, which reduces the initial learning rate α after stated epochs, and while μ signifies the momentum that describes the impact of formerly adjusted weights in the current iteration.

2.5. Transfer learning and Fine tuning of deep models

Different CNN networks possess a varying number of parameters and layers, as depicted in Table 4.

A significant volume of training data is essential for the optimization and training of deep CNN models. Though for a comparatively scantier dataset, it is very difficult to acquire the appropriate local minima for the cost function, represented by Equation 4, due to which the design may encounter overfitting. So, originally, trained parameters are acquired from these deep networks. Then these deep networks are fine-tuned on we fine-tuned COVID19 dataset by using diverse alterations of the learning rate, batch size, and epochs. The primary layers possess generic features, while the succeeding layers maintain domain-related features. To preserve the features from the original layers and reduce the learning rate in the subsequent transfer layers, the primary rate is adjusted to a minimum value. But, to learn more rapidly in the recently attached layers, the learning rate of in recently added fully-connected layer is fixed to a larger value. The fully-connected layer of these models comprises of 1000 neurons, which corresponds to the number of categories in the ImageNet repository. To acquire the domain-rated features, the terminal fully-connected layer is attuned according to categories in the COVID19 dataset. The CNN networks are described as under.

Table **4.** The description of Parameters and Layers for various Pre-trained models

Deep Models	Layers	Parameter
Alex Net	8	60 million
Squeeze Net	18	1.24 million
MobileNet V2	53	3.5 million
DenseNet201	201	20 million

2.5.1. AlexNet

AlexNet was the winner of the 2012 ImageNet competition, which is mainly used for image classification tasks. It can be considered as a wider and deeper variant of LeNet, which includes the primary modules of CNNs, providing the foundation for other deep learning architectures [38]. It preserves the original design but includes more functions such as LRN, dropout, and ReLU. The work's main outcome was that the model's depth was crucial for its huge performance, which was computationally expensive but made possible due to the use of GPUs during training. The model comprises of 5 convolutions, and 3 fully-connected layers, as displayed in in Fig. 2.

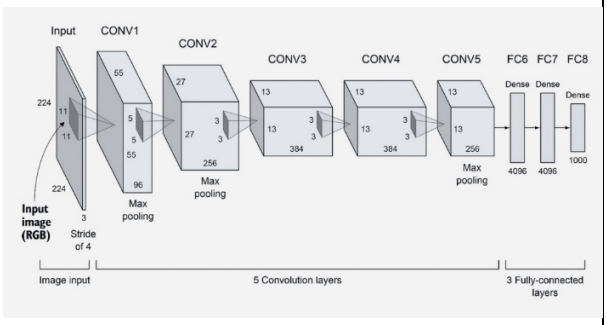

Fig. (2). AlexNet Architecture

2.5.2. SqueezeNet

SqueezeNet is a deep CNN design for image classification that was released in 2016. The model was proposed by researchers at Stanford, Berkeley, and DeepScale [77]. The goal was to create a smaller CNN with lesser parameters that require lesser memory and can quickly be sent over a computer network. The basic building block of this deep model is a fire module, which consists of: a convolution layer comprising of 1x1 filters, feeding into an expand layer that has both 1x1 and 3x3 convolution filters, as shown in Fig. 3.

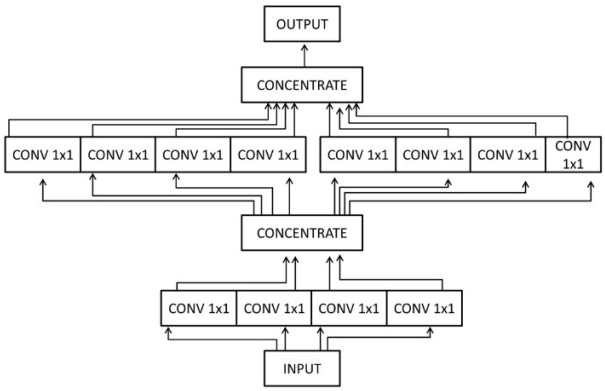

Fig. (3). SqueezeNet Architecture

2.3.3. MobileNetV2

MobileNetV2 is a CNN model that comprises 53 layers. The deep network is a continuation of MobileNetV1, which offers a depth-wise separable convolutional layer, which fantastically decreases the complexity cost and size of the model. The model proposes a further useful module with an inverted residual architecture, where the residual-based connections are among the bottleneck layers. The middle layer is an expanded design that utilizes lightweight depth-wise convolution to separate features. Furthermore, non-linearities are eliminated in the thinner layers to sustain the representational capacity [78]. MobileNetV2 generates excellent performances in object detection, image classification, and semantic segmentation tasks. The Fig.4 displays the MobileNetV2 block diagram.

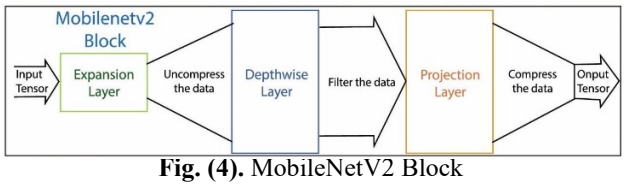

Fig. (4). MobileNetV2 Block

2.5.4. DenseNet

For the proposed deep design, the DenseNet architecture serves as a building block. Dense models require lesser parameters than traditional convolution models as they do not need to learn unnecessary feature-maps. Some disparities in ResNet models were handled and removed in Dense models. ResNet models have large number of parameters, however, DenseNet layers are narrower and they offer new feature-maps in lesser number. RESNET models are difficult to train due to previously reported gradients and data. As layers are connected to the gradients by the loss function and the original image, DenseNet models resolve the problem.

The basic idea of DenseNets is reuse of features, which produces a very compact design. Consequently, the model requires lesser parameters than other deep models as no feature-maps are duplicated. Deeper models, face numerous problems. The issue is mapping of data from the inner layer to the external layer (also the gradient) gets so large that it can disappear before entering any other side. DenseNet models make this connectivity simpler by just combining each layer immediately with every layer. These models take advantage of the model's capability by reusing features. To maximize computational recycling within the classifiers, combining various classification algorithms into an ideal and deep CNN and connects them with dense connections for effective image identification [79]. The study has revealed that CNN's with limited connections within layers and those near to the output can be sustaintially deeper, and will be much more realistic to train [80]. DenseNet delivers substantial enhancements over the other deep learning models while using minimum processing and memory to improve its performance.

In the presented methodology, deep dense block architecture is proposed, which takes the advantage of fine-tuning and data augmentation to further improve the generalizability of the model.

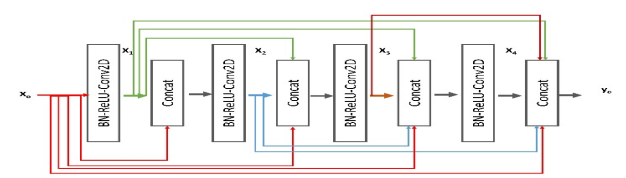

Fig. (5). DenseNet block

3. RESULTS and Discussion

The section demonstrates the experimental outcomes of deep networks besides considering the enhancements these methodologies i.e. (fine-tuning, augmentation, and transfer learning) have brought in the suggested approach. Initially, we select four deep models and apply fine-tuning, augmentation and transfer learning to future improve the performance of these models. We assess the performance of these CNN architectures from two different aspects. When the CNN architectures are (i) augmented and fine-tuned without pre-trained weights and (ii) augmented and fine-tuned with all layers unfrozen. For the methodology, recall, specificity, FScore, and accuracy are computed for CNN models on the COVID19 dataset in Table **5**.

By examining these matrices of models on the COVID19 dataset, we can infer the following conclusions:

1) In most cases, shallow CNN networks generate better results than deeper networks when the dataset is limited. These deeper models possess an enormous number of parameters, which require a significant amount of training data. Previous researches show that shallow networks perform better than deeper networks for image classification tasks [45].

2) Fine-tuning and augmentation strategies are very beneficial for a network's performance when the data is insignificant. Fine-tuning helps models converge speedily and realize domain-specific features. These can also help increase the FScore and accuracy of these CNN designs, even if trained from start during image identification tasks. The outcomes show that the networks only fine-tuned on the augmented COVID19 dataset can considerably improve FScore and accuracy, even if the network is trained from start with any pre-learned weights. Researches also show that fine-tuning a CNN architecture is vital for its reusability

[81]. Current works confirm that fine-tuning is beneficial for various computer vision tasks [82]. Similarly, previous works also maintain that augmentation can help increase the performance and generate more generalized models without overfitting [45, 83].

3) The proposed dense design produces specificity, recall, FScore, and accuracy of 97.33%, 92.01%, 92.00%, and 96.01%, respectively, while employing augmentation and fine-tuning approaches. The design provides improved performance in contrast to any of the CNN architectures. The suggested design accomplished nearly 0.30–1.5% rise in specificity, 0.82–5.1% rise in the recall, 0.89–5% rise in FScore, and 0.41–2.4% rise in accuracy overall the employed CNN models. DenseNet models use dense connections which resolve the issue of vanishing-gradient, substantially reduce the number of parameters, build up feature propagation, and boost feature reuse [80]. Dense models have inspired optimizations in many other deep learning domains like image classification [79], medical diagnosis [84], image segmentation [85], image super-resolution [86] etc.

4) The confusion matrix more elaborates the outcomes of the suggested design for the COVID19 dataset, as given in Figure 5. The Fold-1 matrix reflects that in COVID19, there are only three misclassifications and in the Normal class, there are eight misclassifications. Though, misclassification is comparatively high in the viral and bacterial class (bacterial 26 and viral 48).

5) Overall, the matrices show only five misclassifications for COVID19 and slightly higher (thirty-one) for the Normal class.

Table **5**. An Assessment of several approaches applied on Deep CNN designs. Where, ADS, ALUF, NPTW, FT augmented dataset, all layers un-frozen, no pre-trained weights, fine-tuned.

Model types	**Methods**	**Specificity**	**Recall**	**FScore**	**Accuracy**
Proposed_Model	FT on ADS-NPTW	97.33±0.36	92.01±0.85	92.00±0.87	96.01±0.52
AlexNet	FT on ADS-ALUF	•97.08±0.45	•91.27±1.16	•91.24±1.09	•95.6±0.62
DenseNet201	FT on ADS-ALUF	•96.96+0.90	•90.90+2.80	•91.10+3.03	•95.43+1.36
SqueezNet	FT on ADS-ALUF	•95.87+0.53	•87.59+0.53	•87.62+0.52	•93.80+0.25
MobileNetV2	FT on ADS-ALUF	•97.07+0.59	•91.26+1.49	•91.19+1.57	•95.62+0.84

A • symbolizes that our deep dense model is statistically superior to its contending model.

Overfitting can be an obstacle, especially with modest training examples. A design may attain spectacular performance on the training dataset, but it is sometimes difficult to generate similar results for unseen instances. So, the core issue is to evaluate whether overfitting is observed, or the model shows substantial ability to generalize for the given instances. To perform this assessment, we assess the performance of the design by measuring the gap among the training/validation curves. The greater the space among the curves, the more the overfitting. The training chart in Figure 6 fold-4 of the model, which shows a slight improvement in model's accuracy and loss as the number of epochs increase. The figure also displays that the curves for training and validation overlap, which displays that there is no overfitting and the suggested design can generalize for the training instances.

4. STATISTICAL COMPARISION

For statistical evaluation of the performance of the design against various other deep models, we repeat our evaluation scheme five times. Then, we follow the following steps as given below:

(a) A paired II-sided t-test is applied at 5% significance and compare five accuracies of our design with those of contesting deep architecture.

(b) We hypothesize that difference among accuracies of the suggested design and those of a contesting architecture originates from a normal distribution with variance not known and a zero mean. The other hypothesis is mean is not zero.

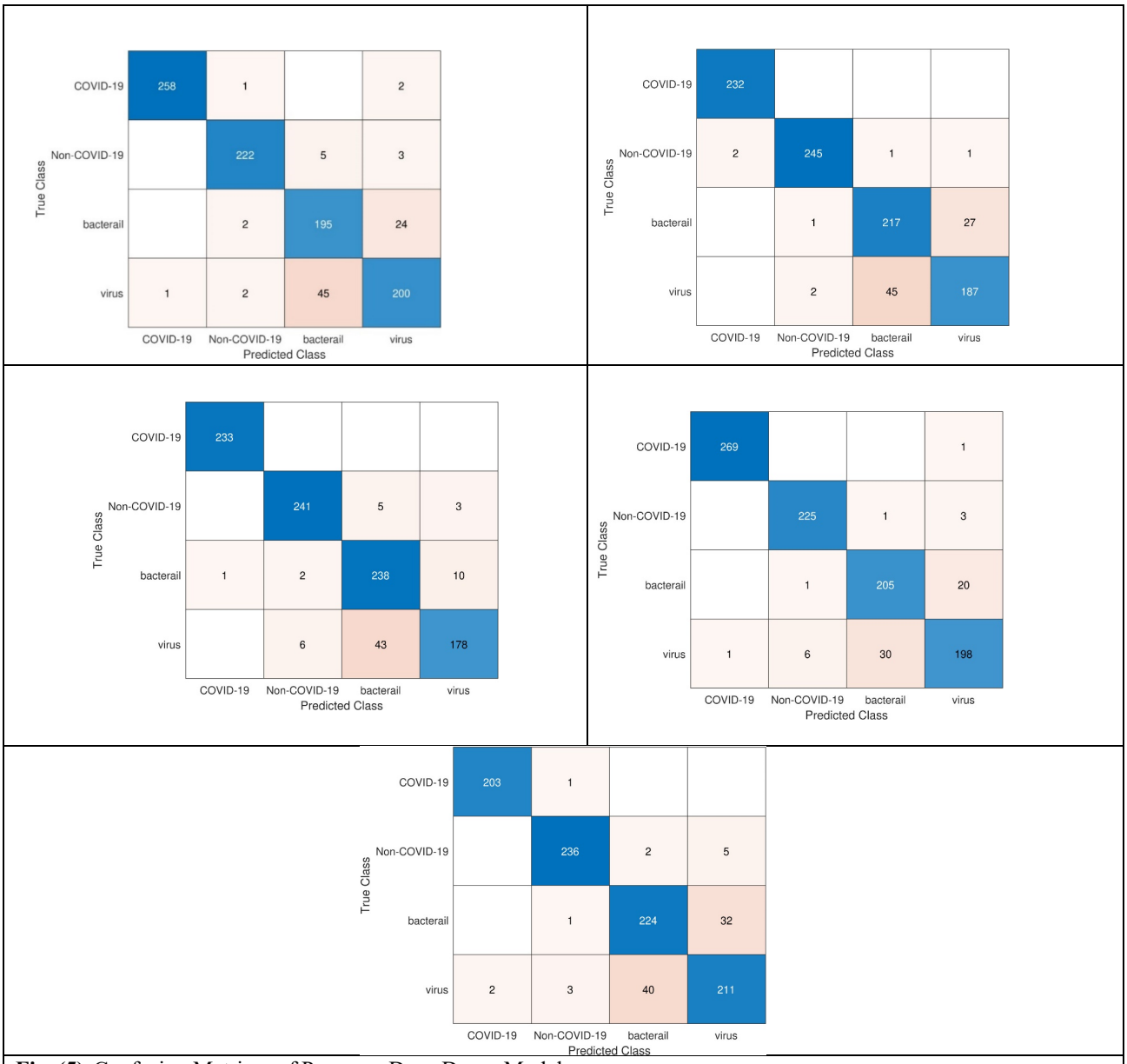

Fig. (5). Confusion Matrices of Proposes Deep Dense Model

Table **6.** Assessment of Proposed deep dense design with current methodologies applied for COVID19 Classification

Approach	**Class**	**Covid-19 Images**	**Hyper-parameter Tuning?**	**5-Folds CV?**	**Balanced Dataset?**	**Statistical Comparison?**	**Accuracy**
Our Proposed Model	4	1200	✓	✓	✓	✓	96.01%
COVID-NET [35]	3	180	×	×	×	×	93.3%
DELT[88]	4	305	×	×	×	×	90.13
CORONET[57]	4	284	×	×	×	×	89.6%
XGB[87]	4	130	×	✓	×	×	79.52%

(c) In case the void hypothesis is declined, the performance of our design is statistically variating from the contesting design. We hold it to be a win for our design if the mean accuracy of the proposed design is higher than that of the contesting design. We represent it be a •. Contrarily, it is a loss for the proposed design. We describe it by a ◦.

(d) In case t-test doesn't reject the void hypothesis, then the performance of the proposed design is not statistically distinct from the contesting design. This will be considered as a tie, shown by no symbol.

The identical statistical analysis scheme applies to recall, specificity, FScores, and accuracy. The outcomes in Table 5 reflect the statistical significance of our design over other competing deep designs.

5. COMPARISON WITH PREVIOUS WORK

We present the comparison of our model with previously employed strategies for the identification of COVID19 in chest X-rays. Initially, the comparison illuminates that the datasets are unbalanced and comprise a limited number of corona +Ve images in all of these strategies. Secondly, cross-validation is used only by few approaches. Finally, hyper-parameter tuning and statistical analysis of deep networks is not employed by any of the techniques. While examining the quality metrics in Table 6, it can be concluded the suggested dense model beats the examined contemporary approaches, attaining an accuracy of 96.01%.

6. Conclusion

In this work, a new COVID-19 classification technique is presented, which applies fine-tuning, data-augmentation, and dense connections for distinguishing between various chest infections. Dense connections resolve the issue of vanishing-gradient, substantially reduce the number of parameters, encourage feature reuse, and strengthen feature propagation. Fine-tuning benefits the design converge rapidly and achieve domain-specific features. The augmentation technique creates diversity among instances of the dataset, which magnifies the generalizability of the design and hence helps in controlling overfitting. The recommended model includes Dense blocks, convolution, and pooling layers, which delivers more reliable classification performance than the examined CNN models. The dense model attains a specificity, recall, FScore, and accuracy of 97.33%, 92.01%, 92.00%, and 96.01%, which can be beneficial for experts in radiology and can also assist diagnostic staff in the correct classification of COVID19 in chest radiographs. Consequently, the dense model can help in the swift and accurate and swift identification of COVID19 patients. As a result, this can limit the socioeconomic impact of the virus on humanity.

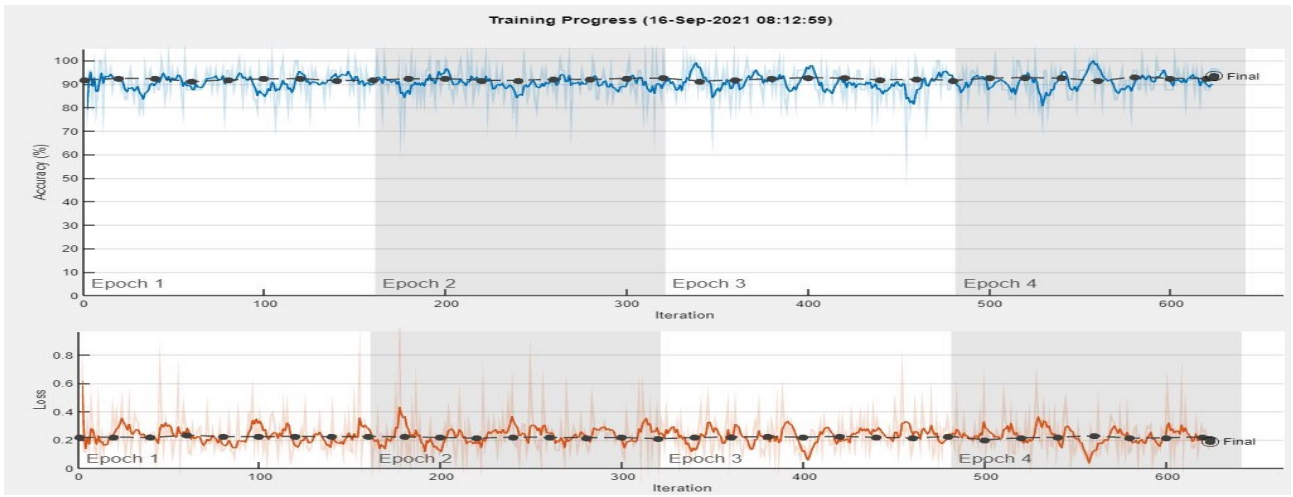

Fig (6). Training chart for training and validation of Fold-4 of fine-tuned Deep dense model, for COVID-19 classification

Conflict of Interest

No interest conflict exists among authors otherwise.

Funding

This project was supported by the deanship of scientific research at Umm AlQura University, Makkah, Saudi Arabia [Grant Code: 20-MED-4-13-0013]

Acknowledgement

Data for this research was provided by the COVID-19 Clinical and Epidemiological Database resource at the King Faisal Specialist Hospital & Research Centre.

References

[1] Ahmad F, Farooq A, Ghani Khan MU, Shabbir MZ, Rabbani M, Hussain I. Identification of most relevant features for classification of Francisella tularensis using machine learning. Current Bioinformatics. 2020 Dec 1;15(10):1197-212.

[2] Salyer SJ, Silver R, Simone K, Behravesh CB. Prioritizing zoonoses for global health capacity building—themes from One Health zoonotic disease workshops in 7 countries, 2014–2016. Emerging infectious diseases. 2017; 23(Suppl 1): S57–S64.

[3] Franconi R, Illiano E, Paolini F, Massa S, Venuti A, Demurtas OC. Rapid and Low-Cost Tools Derived from Plants to Face Emerging/Re-emerging Infectious Diseases and Bioterrorism Agents. In: Defence Against Bioterrorism. Dordrecht: Springer; 2018; pp. 123–39.

[4] Wang H, Naghavi M, Allen C, Barber RM, Bhutta ZA, Carter A, Casey DC, Charlson FJ, Chen AZ, Coates MM, Coggeshall M. Global, regional, and national life expectancy, all-cause mortality, and cause-specific mortality for 249 causes of death, 1980–2015: a systematic analysis for the Global Burden of Disease Study 2015. The lancet. 2016 Oct 8;388(10053):1459-544.

[5] Gebreyes WA, Dupouy-Camet J, Newport MJ, Oliveira CJ, SchlesingerLS, Saif YM, et al. The global one health paradigm: challenges and opportunities for tackling infectious diseases at the human, animal, and environment interface in low-resource settings. PLoS neglected tropical diseases. 2014; 8(11).

[6] Nabarro D, Wannous C. The potential contribution of livestock to food and nutrition security: The application of the One Health approach in livestock policy and practice. Revue scientifique et technique (International Office of Epizootics). 2014; 33(2): 475-485.

[7] Lee PI, Hsueh PR. Emerging threats from zoonotic coronaviruses-from SARS and MERS to 2019-nCoV. Journal of microbiology, immunology, and infection. 2020 Jun;53(3):365.

[8] Cyranoski D. Mystery deepens over animal source of coronavirus. Nature. 2020 Mar 1;579(7797):18-20.

[9] Petherick A. Developing antibody tests for SARS-CoV- 2. The Lancet. 2020 Apr 4;395(10230):1101-2.

[10] King A. The hunt for the next potential coronavirus animal host, https://www.nationalgeographic.com/animals/2020/03/ coronavirus-animal-reservoir-research/, 2020. [Online; accessed 3- April-2020]

[11] World Health Organization. Zoonotic disease: emerging public health threats in the Region, www.emro.who.int/fr/about-who/rc61/zoonotic-diseases.html/, 2008. [Online; accessed 17-July-2011].

[12] Van Doremalen N, Bushmaker T, Morris DH, Holbrook MG, Gamble A, Williamson BN, Tamin A, Harcourt JL, Thornburg NJ, Gerber SI, Lloyd-Smith JO. Aerosol and surface stability of SARS-CoV-2 as compared with SARS-CoV-1. New England journal of medicine. 2020 Apr 16;382(16):1564-7.

[13] World Health Organization. Modes of transmission of virus causing COVID-19: implications for IPC precaution recommendations: scientific brief, 29 March 2020. World Health Organization; 2020

[14] Lewis D. Is the coronavirus airborne? Experts can't agree. Nature. 2020 Apr 9;580(7802):175.

[15] Liu Y, Ning Z, Chen Y, Guo M, Liu Y, Gali NK, Sun L, Duan Y, Cai J, Westerdahl D, Liu X. Aerodynamic characteristics and RNA concentration of SARS-CoV-2 aerosol in Wuhan hospitals during COVID-19 outbreak. bioRxiv. 2020. Google Scholar. 2020

[16] Cheng VC, Wong SC, Chen JH, Yip CC, Chuang VW, Tsang OT, Sridhar S, Chan JF, Ho PL, Yuen KY. Escalating infection control response to the rapidly evolving epidemiology of the coronavirus disease 2019 (COVID-19) due to SARS-CoV-2 in Hong Kong. Infection Control & Hospital Epidemiology. 2020 May;41(5):493-8.

[17] Watts E, Leck A, Hu V. Personal protective equipment for COVID-19 in eye care. Community Eye Health. 2020;33(109):28

[18] Bourouiba L. Turbulent gas clouds and respiratory pathogen emissions: potential implications for reducing transmission of COVID-19. Jama. 2020 May 12;323(18):1837-8

[19] COVID C. global cases by the Center for Systems Science and Engineering (CSSE) at Johns Hopkins University (JHU). johns hopkins coronavirus resource center, vol. 19.

[20] Dehghani A, Masoumi G. Could sars-cov-2 or covid-19 be a biological weapon?. Iranian Journal of Public Health. 2020 Oct;49(Suppl 1):143.

[21] Khurshid SJ. Novel Coronavirus (nCoV-2019): Is it a Bioweapon. J. Bioterror. Biodef. 2020;11:166.

[22] C. for Systems Science, Engineering, Covid-19 dashboard by the center for systems science and engineering (csse) at johns hopkins university (jhu), https://coronavirus.jhu.edu/map.html/, 2021. [Online; accessed 30- September-2021.

[23] Shear MD, Crowley M, Glanz J. Coronavirus may kill 100,000 to 240,000 in US despite actions, officials say. officials say, https://www.nytimes.com/2020/03/31/us/politics/coronavirus-death-toll-united-states.html/, 2020. [Online; accessed 31-March-2020].

[24] Lintern S. Coronavirus could kill half a million Britons and infect 80% of UK population, government documents indicate, https://www.independent.co.uk/news/health/ coronavirus-news-latest-deaths-uk-infection-flu-a9360271. html/, 2020. [Online; accessed 26-February-2020].

[25] Sadegh N, Sadegh P. Test-Based Stabilizing Control of COVID-19 Transmission.

[26] cdc gov, Food safety, 2019.

[27] Menachery VD, Graham RL, Baric RS. Jumping species—a mechanism for coronavirus persistence and survival. Current opinion in virology. 2017 Apr 1;23:1-7.

[28] Ai T, Yang Z, Hou H, Zhan C, Chen C, Lv W, Tao Q, Sun Z, Xia L. Correlation of chest CT and RT-PCR testing for coronavirus disease 2019 (COVID-19) in China: a report of 1014 cases. Radiology. 2020 Aug;296(2):E32-40.

[29] Kolifarhood G, Aghaali M, Saadati HM, Taherpour N, Rahimi S, Izadi N, Nazari SS. Epidemiological and clinical aspects of COVID-19; a narrative review. Archives of academic emergency medicine. 2020;8(1).

[30] Oh Y, Park S, Ye JC. Deep learning covid-19 features on cxr using limited training data sets. IEEE transactions on medical imaging. 2020 May 8;39(8):2688-700.

[31] Xie X, Zhong Z, Zhao W, Zheng C, Wang F, Liu J. Chest CT for typical coronavirus disease 2019 (COVID-19) pneumonia: relationship to negative RT-PCR testing. Radiology. 2020 Aug;296(2):E41-5.

[32] Fang Y, Zhang H, Xie J, Lin M, Ying L, Pang P, Ji W. Sensitivity of chest CT for COVID-19: comparison to RT-PCR. Radiology. 2020 Aug;296(2):E115-7.

[33] Ng, Ming-Yen, et al. "Imaging profile of the COVID-19 infection: radiologic findings and literature review." Radiology: Cardiothoracic Imaging 2.1 (2020): e200034.

[34] Huang C, Wang Y, Li X, Ren L, Zhao J, Hu Y, Zhang L, Fan G, Xu J, Gu X, Cheng Z. Clinical features of patients infected with 2019 novel coronavirus in Wuhan, China. The lancet. 2020 Feb 15;395(10223):497-506.

[35] Wang L, Lin ZQ, Wong A. Covid-net: A tailored deep convolutional neural network design for detection of covid-19 cases from chest x-ray images. Scientific Reports. 2020 Nov 11;10(1):1-2.

[36] Ahmad F, Khan MU, Javed K. Deep learning model for distinguishing novel coronavirus from other chest related infections in X-ray images. Computers in biology and medicine. 2021 Jul 1;134:104401.

[37] Szegedy C, Vanhoucke V, Io_e S, Shlens J, Wojna Z. Rethinking the inception architecture for computer vision. In: Proceedings of the IEEE conference on computer vision and pattern recognition; 2016; pp. 2818-2826.

[38] Krizhevsky A, Sutskever I, Hinton GE. ImageNet classification with deep convolutional neural networks. Communications of the ACM. 2017 May 24;60(6):84-90.

[39] Deng J, Dong W, Socher R, Li LJ, Li K, Fei-Fei L. Imagenet: A large-scale hierarchical image database. In2009 IEEE conference on computer vision and pattern recognition 2009 Jun 20 (pp. 248-255). Ieee.

[40] Sermanet P, Frome A, Real E. Attention for fine-grained categorization. arXiv preprint arXiv:1412.7054. 2014 Dec 22

[41] Ahmad F, Farooq A, Ghani MU. Deep ensemble model for classification of novel coronavirus in chest X-ray images. Computational intelligence and neuroscience. 2021 Jan 5;2021

[42] Dawud AM, Yurtkan K, Oztoprak H. Application of deep learning in neuroradiology: brain haemorrhage classification using transfer learning. Computational Intelligence and Neuroscience. 2019 Jun 3;2019.

[43] Ahmad F, Farooq A, Khan MU. Deep Learning Model for Pathogen Classification Using Feature Fusion and Data Augmentation. Current Bioinformatics. 2021 Mar 1;16(3):466-83.

[44] Russakovsky O, Deng J, Su H, Krause J, Satheesh S, Ma S, Huang Z, Karpathy A, Khosla A, Bernstein M, Berg AC. Imagenet large scale visual recognition challenge. International journal of computer vision. 2015 Dec;115(3):211-52.

[45] Han D, Liu Q, Fan W. A new image classification method using CNN transfer learning and web data augmentation. Expert Systems with Applications. 2018 Apr 1;95:43-56.

[46] Aneja N, Aneja S. Transfer learning using CNN for handwritten devanagari character recognition. In2019 1st International Conference on Advances in Information Technology (ICAIT) 2019 Jul 25 (pp. 293-296). IEEE.

[47] Lakhani P, Sundaram B. Deep learning at chest radiography: automated classification of pulmonary tuberculosis by using convolutional neural networks. Radiology. 2017 Aug;284(2):574-82.

[48] Huang P, Park S, Yan R, Lee J, Chu LC, Lin CT, Hussien A, Rathmell J, Thomas B, Chen C, Hales R. Added value of computer-aided CT image features for early lung cancer diagnosis with small pulmonary nodules: a matched case-control study. Radiology. 2018 Jan;286(1):286-95.

[49] Cohen JP, Morrison P, Dao L, Roth K, Duong TQ, Ghassemi M. Covid-19 image data collection: Prospective predictions are the future. arXiv preprint arXiv:2006.11988. 2020 Jun 22.

[50] Gozes O, Frid-Adar M, Greenspan H, Browning PD, Zhang H, Ji W, Bernheim A, Siegel E. Rapid ai development cycle for the coronavirus (covid-19) pandemic: Initial results for automated detection & patient monitoring using deep learning ct image analysis. arXiv preprint arXiv:2003.05037. 2020 Mar 10.

[51] Xu X, Jiang X, Ma C, Du P, Li X, Lv S, Yu L, Ni Q, Chen Y, Su J, Lang G. A deep learning system to screen novel coronavirus disease 2019 pneumonia. Engineering. 2020 Oct 1;6(10):1122-9.

[52] Wang S, Kang B, Ma J, Zeng X, Xiao M, Guo J, Cai M, Yang J, Li Y, Meng X, Xu B. A deep learning algorithm using CT images to screen for Corona Virus Disease (COVID-19). European radiology. 2021 Feb 24:1-9.

[53] Gozes O, Frid-Adar M, Greenspan H, Browning PD, Zhang H, Ji W, Bernheim A, Siegel E. Rapid ai development cycle for the coronavirus (covid-19) pandemic: Initial results for automated detection & patient monitoring using deep learning ct image analysis. arXiv preprint arXiv:2003.05037. 2020 Mar 10.

[54] Apostolopoulos ID, Mpesiana TA. Covid-19: automatic detection from x-ray images utilizing transfer learning with convolutional neural networks. Physical and Engineering Sciences in Medicine. 2020 Jun;43(2):635-40.

[55] Ucar F, Korkmaz D. COVIDiagnosis-Net: Deep Bayes-SqueezeNet based diagnosis of the coronavirus disease 2019 (COVID-19) from X-ray images. Medical hypotheses. 2020 Jul 1;140:109761.

[56] Abbas A, Abdelsamea MM, Gaber MM. Classification of COVID-19 in chest X-ray images using DeTraC deep convolutional neural network. Applied Intelligence. 2021 Feb;51(2):854-64.

[57] Khan AI, Shah JL, Bhat MM. CoroNet: A deep neural network for detection and diagnosis of COVID-19 from chest x-ray images. Computer Methods and Programs in Biomedicine. 2020 Nov 1;196:105581.

[58] Afshar P, Heidarian S, Naderkhani F, Oikonomou A, Plataniotis KN, Mohammadi A. Covid-caps: A capsule network-based framework for identification of covid-19 cases from x-ray images. Pattern Recognition Letters. 2020 Oct 1;138:638-43.

[59] Gianchandani N, Jaiswal A, Singh D, Kumar V, Kaur M. Rapid COVID-19 diagnosis using ensemble deep transfer learning models from chest radiographic images. Journal of ambient intelligence and humanized computing. 2020 Nov 16:1-3.

[60] Singh D, Kumar V, Yadav V, Kaur M. Deep neural network-based screening model for COVID-19-infected patients using chest X-ray images. International Journal of Pattern Recognition and Artificial Intelligence. 2021 Mar 15;35(03):2151004.

[61] Singh D, Kumar V, Kaur M. Densely connected convolutional networks-based COVID-19 screening model. Applied Intelligence. 2021 May;51(5):3044-51.

[62] Luz E, Silva P, Silva R, Silva L, Guimarães J, Miozzo G, Moreira G, Menotti D. Towards an effective and efficient deep learning model for COVID-19 patterns detection in X-ray images. Research on Biomedical Engineering. 2021 Apr 20:1-4.

[63] Khobahi S, Agarwal C, Soltanalian M. Coronet: A deep network architecture for semi-supervised task-based identification of covid-19 from chest x-ray images. MedRxiv. 2020 Jan 1.

[64] Rajaraman S, Siegelman J, Alderson PO, Folio LS, Folio LR, Antani SK. Iteratively pruned deep learning ensembles for COVID-19 detection in chest X-rays. IEEE Access. 2020 Jun 19;8:115041-50.

[65] Minaee S, Kafieh R, Sonka M, Yazdani S, Soufi GJ. Deep-covid: Predicting covid-19 from chest x-ray images using deep transfer learning. Medical image analysis. 2020 Oct 1;65:101794.

[66] Farooq M, Hafeez A. Covid-resnet: A deep learning framework for screening of covid19 from radiographs. arXiv preprint arXiv:2003.14395. 2020 Mar 31.

[67] Chowdhury ME, Rahman T, Khandakar A, Mazhar R, Kadir MA, Mahbub ZB, Islam KR, Khan MS, Iqbal A, Al Emadi N, Reaz MB. Can AI help in screening viral and COVID-19 pneumonia?. IEEE Access. 2020 Jul 20;8:132665-76.

[68] Flusser J, Suk T. Character recognition by affine moment invariants. InInternational Conference on Computer Analysis of Images and Patterns 1993 Sep 13 (pp. 572-577). Springer, Berlin, Heidelberg.

[69] Rahman T, Chowdhury ME, Khandakar A, Islam KR, Islam KF, Mahbub ZB, Kadir MA, Kashem S. Transfer learning with deep convolutional neural network (CNN) for pneumonia detection using chest X-ray. Applied Sciences. 2020 Jan;10(9):3233.

[70] Asraf, A; Islam, Z (2021), "COVID19, Pneumonia and Normal Chest X-ray PA Dataset", Mendeley Data, V1, doi: 10.17632/jctsfj2sfn.1

[71] Boghdadi, MA(2021), "COVID19 Chest X-ray PA Dataset", King Faisal Specialist Hospital and Research Centre (KFSH&RC) Jeddah, Kingdom of Saudi Arabia.

[72] SIRM. COVID-19 database. Society of Medical and Interventional Radiology; 2021. Accessed 3 June 2021. Available from: https://www.sirm.org/category/senza-categoria/covid-19/.

[73] Radiopaedia. Radiopaedia; 2021. Accessed 7 June 2021. Available from: https://radiopaedia.org/.

[74] Mitchell TM, et al. Machine learning. 1997. Burr Ridge, IL: McGraw Hill. 1997; 45(37): 870-877.

[75] Swati ZN, Zhao Q, Kabir M, Ali F, Ali Z, Ahmed S, Lu J. Brain tumor classification for MR images using transfer learning and fine-tuning. Computerized Medical Imaging and Graphics. 2019 Jul 1;75:34-46.

[76] Swati ZN, Zhao Q, Kabir M, Ali F, Ali Z, Ahmed S, Lu J. Content-based brain tumor retrieval for MR images using transfer learning. IEEE Access. 2019 Jan 14;7:17809-22.

[77] Iandola FN, Han S, Moskewicz MW, Ashraf K, Dally WJ, Keutzer K. SqueezeNet: AlexNet-level accuracy with 50x fewer parameters and< 0.5 MB model size. arXiv preprint arXiv:1602.07360. 2016 Feb 24.

[78] Sandler M, Howard A, Zhu M, Zhmoginov A, Chen LC. Mobilenetv2: Inverted residuals and linear bottlenecks. InProceedings of the IEEE conference on computer vision and pattern recognition 2018 (pp. 4510-4520).

[79] Huang G, Chen D, Li T, Wu F, van der Maaten L, Weinberger KQ. Multi-scale dense networks for resource efficient image classification. arXiv preprint arXiv:1703.09844. 2017 Mar 29.

[80] Huang G, Liu Z, Van Der Maaten L, Weinberger KQ. Densely connected convolutional networks. InProceedings of the IEEE conference on computer vision and pattern recognition 2017 (pp. 4700-4708).

[81] Yosinski J, Clune J, Bengio Y, Lipson H. How transferable are features in deep neural networks?. arXiv preprint arXiv:1411.1792. 2014 Nov 6.

[82] Shin HC, Roth HR, Gao M, Lu L, Xu Z, Nogues I, Yao J, Mollura D, Summers RM. Deep convolutional neural networks for computer-aided detection: CNN architectures, dataset characteristics and transfer learning. IEEE transactions on medical imaging. 2016 Feb 11;35(5):1285-98.

[83] Jin J, Dundar A, Culurciello E. Flattened convolutional neural networks for feedforward acceleration. arXiv preprint arXiv:1412.5474. 2014 Dec 17.

[84] Chauhan T, Palivela H, Tiwari S. Optimization and Fine-Tuning of DenseNet model for classification of Covid-19 cases in Medical Imaging. International Journal of Information Management Data Insights. 2021 Jun 10:100020.

[85] Kohl M, Walz C, Ludwig F, Braunewell S, Baust M. Assessment of breast cancer histology using densely connected convolutional networks. InInternational Conference Image Analysis and Recognition 2018 Jun 27 (pp. 903-913). Springer, Cham.

[86] Kuang P, Ma T, Chen Z, Li F. Image super-resolution with densely connected convolutional networks. Applied Intelligence. 2019 Jan;49(1):125-36.

[87] Hussain L, Nguyen T, Li H, Abbasi AA, Lone KJ, Zhao Z, Zaib M, Chen A, Duong TQ. Machine-learning classification of texture features of portable chest X-ray accurately classifies COVID-19 lung infection. BioMedical Engineering OnLine. 2020 Dec;19(1):1-8.

[88] Basu S, Mitra S, Saha N. Deep learning for screening covid-19 using chest x-ray images. In2020 IEEE Symposium Series on Computational Intelligence (SSCI) 2020 Dec 1 (pp. 2521-2527). IEEE.

Wesam H. Alsabban received the B.Sc. degree in electrical and computer engineering from Umm Al-Qura University, Makkah, Saudi Arabia, in 2000, and the M.Sc. and PhD degrees in engineering systems from Queensland University of Technology, Brisbane, Australia, in 2009 and 2014, respectively. Currently Dr. Wesam is an Assistant Professor in the Computer Engineering department at Umm Al-Qura University, Makkah, Saudi Arabia. His research interests include artificial intelligent, robotic, and deep learning.

Fareed Ahmad received the PhD degree in Computer Science from University of Engineering and Technology Lahore, Pakistan in 2021. Currently Dr. Fareed is working at the Institute of Microbiology, Quality Operations Laboratory, University of Veterinary and Animal Sciences, Lahore, Pakistan. His research interests include artificial intelligent, image processing, and deep learning.

Ali Al-Laith received the PhD degree in Computer Science from University of Engineering and Technology Lahore, Pakistan. Currently Dr. Ali is working as a research associate at the Center for Language Engineering, KICS, UET Lahore, Pakistan. His research interests include artificial intelligent, natural language processing, and machine learning.

Saeed M. Kabrah is working at the Laboratory Medicine Department, Umm Al-Qura University, Makkah Al Mukarramah, Saudi Arabia.

Mohammed A. Baghdadi is working at King Faisal Specialist Hospital and Research Centre, Jeddah, Saudi Arabia.

Farhan Masud is currently an Assistant Professor, Department of Statistics and Computer Science. He received M.Sc. degree in Computer Science (1999) from Quaid-i-Azam University Islamabad, MS in Computer Science (2014) from Government College University (Pakistan) and PhD degree (2019) from Universiti Teknologi Malaysia (Malaysia).